NON LINEAR DYNAMICS STUDY OF THE CLIC DAMPING RINGS USING SYMPLECTIC INTEGRATORS

Ch. Skokos*, IMCCE–Observatoire de Paris, Paris, France and
Max Planck Institute for the Physics of Complex Systems, Dresden, Germany
Y. Papaphilippou, CERN, Geneva, Switzerland

Abstract

A class of symplectic integrators with positive steps ($SABA_2$) is applied to investigate the non-linear dynamics of the CLIC damping rings. The detrimental effect of the chromaticity sextupoles is studied using frequency and diffusion maps and verified with MADX ptc dynamic aperture tracking. The reduction of the dynamic aperture for off-momentum particles is also investigated.

THE $SABA_2$ SYMPLECTIC INTEGRATOR

Symplectic integrators are extensively used for single particle tracking in accelerators. A symplectic integrator scheme, which involves only positive steps, for perturbed Hamiltonians of the form $H = A + \epsilon B$, where both A and B are integrable, was proposed [1], and all order of such integrators were derived [2]. A particular member of the family, namely the $SABA_2$ integrator has already proved to be very efficient for the numerical study of astronomical [2], as well as accelerator models [3, 4].

An orbit of a Hamiltonian system of N degrees of freedom $H(\vec{p},\vec{q})$, with $\vec{p} = (p_1,\ldots,p_N)$, $\vec{q} = (q_1,\ldots,q_N)$ and q_i, p_i, $i = 1,\ldots,N$ the generalized coordinates and momenta respectively, is defined by a vector $\vec{x}(t) = (x_1(t),\ldots,x_{2N}(t))$, with $x_i = p_i$, $x_{i+N} = q_i$, $i = 1,\ldots,N$. Defining the Poisson bracket of functions $f(\vec{p},\vec{q})$, $g(\vec{p},\vec{q})$ by:

$$\{f,g\} = \sum_{i=1}^{N}\left(\frac{\partial f}{\partial p_i}\frac{\partial g}{\partial q_i} - \frac{\partial f}{\partial q_i}\frac{\partial g}{\partial p_i}\right), \qquad (1)$$

the Hamilton equations of motion take the form:

$$\frac{d\vec{x}}{dt} = \{H,\vec{x}\} = L_H\vec{x}, \qquad (2)$$

where L_H is the differential operator defined by $L_\chi f = \{\chi, f\}$. The solution of Eq. (2), for initial conditions $\vec{x}(0) = \vec{x}_0$, is formally written as $\vec{x}(t) = \sum_{n\geq 0}\frac{t^n}{n!}L_H^n\vec{x}_0 = e^{tL_H}\vec{x}_0$. A symplectic scheme for integrating (2) from t to $t+\tau$ consists of approximating in a symplectic way the operator $e^{\tau L_H} = e^{\tau(L_A+L_{\epsilon B})}$ by an integrator of n steps involving products of $e^{c_i\tau L_A}$ and $e^{d_i\tau L_{\epsilon B}}$, $i = 1,\ldots,n$, which are exact integrations over $c_i\tau$ and $d_i\tau$ of the integrable Hamiltonians A and B. The constants c_i, d_i, are chosen so that to increase the order of the remainder of this approximation. For the $SABA_2$ integrator we get:

$$SABA_2 = e^{c_1\tau L_A}e^{d_1\tau L_{\epsilon B}}e^{c_2\tau L_A}e^{d_1\tau L_{\epsilon B}}e^{c_1\tau L_A}, \qquad (3)$$

with $c_1 = \frac{1}{2}(1-\frac{1}{\sqrt{3}})$, $c_2 = \frac{1}{\sqrt{3}}$, $d_1 = \frac{1}{2}$. Using the $SABA_2$ integrator we are actually approximating the dynamical behavior of the real Hamiltonian $A+\epsilon B$ by a Hamiltonian $K = A + \epsilon B + O(\tau^4\epsilon + \tau^2\epsilon^2)$, i. e. introducing an error term of the order $\tau^4\epsilon + \tau^2\epsilon^2$.

The accuracy of the $SABA_2$ integrator can be improved when the term $C = \{\{A,B\},B\}$ leads to an integrable system, as in the common situation of A being quadratic in actions $\vec{p}$ and B depending only on positions $\vec{q}$. In this case, two correctors can be added with small negative steps:

$$SABA_2C = e^{-\tau^3\epsilon^2\frac{c}{2}L_C}(SABA_2)e^{-\tau^3\epsilon^2\frac{c}{2}L_C}. \qquad (4)$$

The value of $c = (2-\sqrt{3})/2$ was chosen in order to eliminate the $\tau^2\epsilon^2$ dependence of the remainder which becomes of order $O(\tau^4\epsilon+\tau^4\epsilon^2)$. We note that the $SABA_2$ integrator involves only positive steps which increases its numerical stability, while, the addition of the corrector results to better accuracy of the scheme, introducing simultaneously a small negative step. The accuracy of the $SABA_2C$ integrator was studied in [3, 4] where it was shown that it is very precise with a precision one order of magnitude higher than the Forrest and Ruth 4th order integrator [5].

We also note that the usual 'drift–kick' integrator, which is quite commonly used in accelerator tracking, corresponds to the 2nd order symplectic integrator $SABA_1 = e^{\frac{\tau}{2}L_A}e^{\tau L_{\epsilon B}}e^{\frac{\tau}{2}L_A}$, having a remainder of order $O(\tau^2\epsilon)$.

The accelerator Hamiltonian in 'hard edge' and 'small angles' approximation is written as

$$H(x,y,l,p_x,p_y,\delta;s) = H_0 + V \qquad (5)$$

with the unperturbed part $H_0 = (1+h(s)x)\frac{p_x^2+p_y^2}{2(1+\delta)}$, and the perturbation written as a power series

$$V = \sum_{n\geq 1}\sum_{j=0}^{n} a_{n,j}(s)x^j y^{n-j}, \qquad (6)$$

where $a_{n,j}(s)$ are appropriate path dependent constants. The Hamiltonian (5) is suitable for the implementation of the $SABA_2C$ integrator scheme ($A \equiv H_0$, $B \equiv V$, $\epsilon = 1$). The corresponding Hamilton equations of motion for the unperturbed part of the Hamiltonian are

$$\begin{array}{ll} \frac{dx}{ds} = \frac{(1+hx)p_x}{1+\delta}, & \frac{dp_x}{ds} = -\frac{h\left(p_x^2+p_y^2\right)}{2(1+\delta)} \\ \frac{dy}{ds} = \frac{(1+hx)p_y}{1+\delta}, & \frac{dp_y}{ds} = 0 \end{array}. \qquad (7)$$

* Supported by the Marie Curie Intra–European Fellowship No MEIF–CT–2006–025678

Assuming that $p_y^i \neq 0$ and $(1+hx^i)(1+hx^f) > 0$, which is true for real accelerators since usually $|hx| \ll 1$, the following solution can be derived [3, 6]:

$$e^{sL_A}: \begin{cases} x^f = \frac{1}{h}\left[(1+hx^i)(\cos\phi + \frac{p_x^i}{p_y^i}\sin\phi)^2 - 1\right] \\ y^f = y^i + \frac{1+hx^i}{h}\left[\frac{{p_x^i}^2 + {p_y^i}^2}{{p_y^i}^2}\phi + \right. \\ \qquad \left. \frac{{p_y^i}^2 - {p_x^i}^2}{2{p_y^i}^2}\sin(2\phi) + 2\frac{p_x^i}{p_y^i}\sin^2\phi\right] \\ p_x^f = p_y^i \frac{p_x^i - p_y^i\tan\phi}{p_y^i + p_x^i\tan\phi} \\ p_y^f = p_y^i \end{cases}, \quad (8)$$

where $\phi = \frac{p_y^i hs}{2(1+\delta)}$ and superscripts i, f denote respectively the coordinates at the entence and the exit of an element. As the perturbation does not depend on the momenta p_x, p_y it is easily shown that the operator e^{sL_B} $(B \equiv V)$ is:

$$e^{sL_B}: \begin{cases} x^f = x^i, \quad p_x^f = p_x^i - \left.\frac{\partial V}{\partial x}\right|_i s \\ y^f = y^i, \quad p_y^f = p_y^i - \left.\frac{\partial V}{\partial y}\right|_i s \end{cases}, \quad (9)$$

where

$$\begin{aligned} \left.\frac{\partial V}{\partial x}\right|_i &= \sum_{n\geq 1}\sum_{j=1}^{n} j a_{n,j}(x^i)^{j-1}(y^i)^{n-j} \\ \left.\frac{\partial V}{\partial y}\right|_i &= \sum_{n\geq 1}\sum_{j=0}^{n}(n-j) a_{n,j}(x^i)^{j}(y^i)^{n-j-1} \end{aligned}, \quad (10)$$

are the first partial derivatives of $V(x,y)$ with respect to x and y, evaluated at the initial point x^i, y^i.

In order for the corrector operator e^{sL_C} to be applicable the double Poisson bracket $C = \{\{A,B\},B\}$ should determine an integrable system. For $A = H_0$ and $B = V(x,y)$:

$$\{\{A,B\},B\} = \frac{1+hx}{1+\delta}\left[\left(\frac{\partial V}{\partial x}\right)^2 + \left(\frac{\partial V}{\partial y}\right)^2\right], \quad (11)$$

which is a function of only the positions x and y corresponding to an integrable system, leading to the corrector scheme whose expression can be computed explicitly [6].

CLIC DAMPING RINGS

The CLIC damping rings are composed of two arcs with theoretical minimum emittance (TME) cells and long straight sections filled with super-conducting wigglers [7]. Their latest parameters can be found in [8]. In order for the TME cells to achieve an ultra-low emittance, a high-phase advance per cell is necessary which eventually leads to a high chromaticity and small dispersion and thereby to chromaticity sextupole strengths which are high, reducing the dynamic aperture (DA). This is confirmed also in Fig. 1, where the 1000-turns DA of the CLIC damping rings is plotted. The 5D tracking is performed with MADX-ptc [9] and the only non-linearities included are the two sextupoles families, the strength of which is tuned to set for chromaticity equal to zero. The wigglers are modeled as a series of small dipoles with opposite polarity. The on-momentum horizontal DA is quite small and equal to around $3\sigma_x$ whereas the vertical one is larger (around $8\,\sigma_y$). For off-momentum particles of $\pm 0.5\%$, the situtation remains unchanged for the horizontal aperture but the vertical one reduces by around $2\sigma_y$. Note also that for the negative momentum spread the DA appears even smaller.

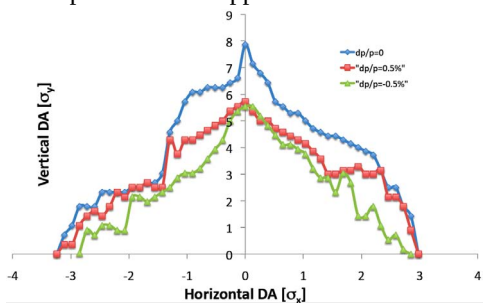

Figure 1: 1000-turns 5D Dynamics aperture for on (blue) and off momentum particles of + (red) and - (green) 0.5%.

A frequency map for the on-momentum dynamics is produced using the SABA$_2$C symplectic integrator modeling the CLIC damping rings (Fig. 2). The tracking is done for 1200 turns and the color coding corresponds to the frequency diffusion coefficient, defined by the logarithm of the frequency vector variation in two consecutive time-spans (blue for stable, red for chaotic motion). Although the particles are tracked for both positive and negative initial horizontal amplitudes, the frequency map corresponding to positive amplitudes is presented here, as the complementary one is very similar. The symplectic integrator reproduces with a good precision the linear tunes of (69.84,33.80). The map shows that the detuning with amplitude is unbalanced between the two planes, giving a huge tune-shift in the vertical, for high horizontal amplitudes, and an order of magnitude smaller in the horizontal (for vertical amplitudes). This means that the cross term of the first order tune-shift with amplitude is quite big. For this reason there is a multitude of vertical resonances crossed like $\nu_y = 33.67$ and $\nu_y = 33.75$. As the superperiodicity of the ring is just 2, these resonances should correspond to the systematic 6th (0,6) and 8th order (0,8). The first one does not appear only for $\nu_y = 33.67$, but also for $\nu_y = 33.83$, in the upper left part of the frequency map, whereas the second one appears also in $\nu_y = 33.80$ on top of the working point. This line corresponds also to the systematic vertical 5th order resonance (0,5), which also appears at the right bottom corner of the map, as $\nu_y = 33.5$.

A complementary information about the dynamics of the system is the diffusion map of Fig. 3 where the real transverse space (x,y) is mapped with the frequency diffusion coefficient. The resonant lines are visible as light colored

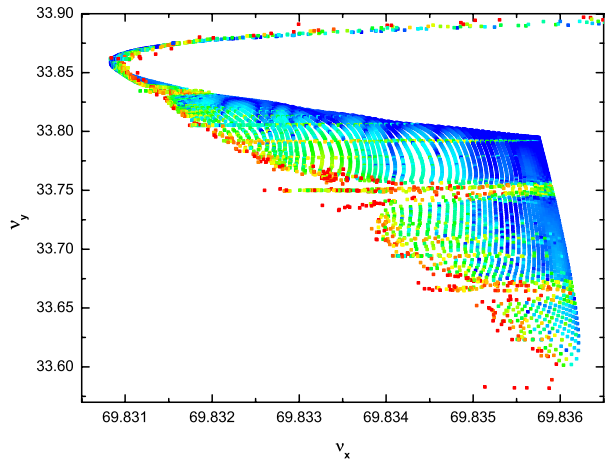

Figure 2: Frequency map for on-momentum particles of the CLIC damping ring.

curves penetrating into the "blue see" of stable motion. It is important to stress that the DA is very close to the one obtained the MADX-ptc tracking, ranging from 60 μm in the horizontal plane, which corresponds to 3 σ_x for a beam size of 20 μm, to 50 μm in the vertical plane, corresponding to around 8 σ_y, for a vertical beam size of 6.3 μm, for the injected normalized emittances of 63 μm.rad and 1.5 μm.rad, respectively. The diffusion map reproduces as well the reduction of the DA for horizontal amplitudes as compared to the positive ones.

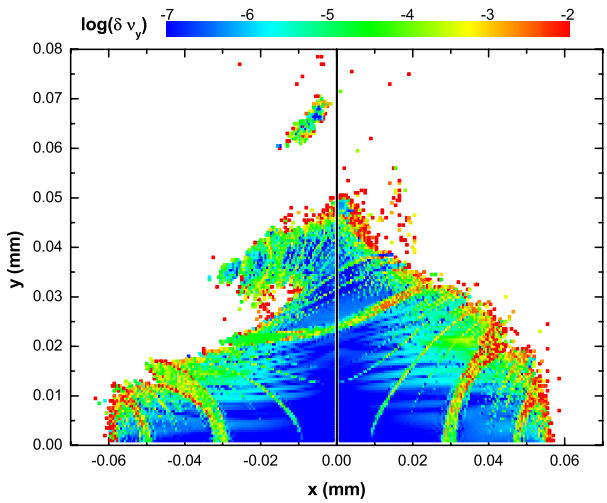

Figure 3: Diffusion map for on-momentum particles of the CLIC damping ring.

In Fig. 4, the frequency map is presented for particles with momentum spread of +0.5%. Even if the sextupoles strengths are tuned to eliminate chromaticity in MADX and then fed to the symplectic tracking code, there is a large tune-shift with momentum. MADX includes the effect of dipoles fringe fields which are predominantly sextupole-like and contribute to chromaticity. This may be amplified by modeling the wigglers as a series of small dipoles with alternating polarity. On the other hand, the symplectic tracking code does not include fringe-field effects and this can explain the observed discrepancy. The above mentioned observation about the tune-shift with amplitude remains. The diffusion maps in Fig. 5 for momentum spread of $\pm 0.5\%$ indicate the reduction of the DA especially in the negative case, as it was observed in the MADX-ptc tracking but the comparison can not be conclusive due to the difference in chromaticity with MADX-ptc.

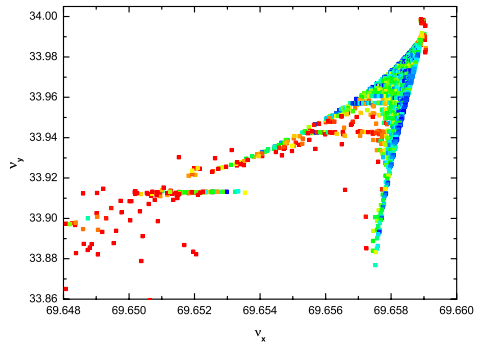

Figure 4: Frequency map for particles with momentum spread of +0.5%.

In conclusion, the symplectic integrator SABA$_2$C combined with frequency map analysis are proved to be robust tools for analyzing the CLIC damping rings nonlinear dynamics. The agreement between the integrator and MADX-ptc is quite good for on-momentum particles. The next steps is the inclusion of fringe-field effects which will alleviate the discrepancy in the chromaticity, the correct modeling of the wigglers and introduction of non-interleaved schemes with more sextupole families.

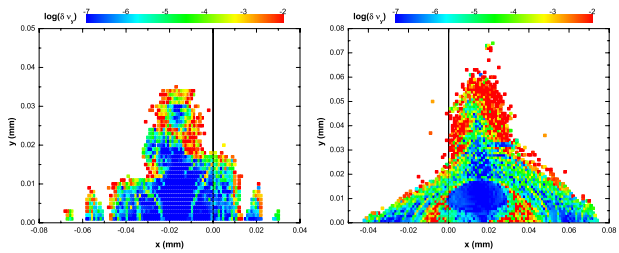

Figure 5: Diffusion map for particles with momentum spread of +0.5% (left) and -0.5% (right).

REFERENCES

[1] R. I. McLachan, BIT Num. Math., 35(2), 258, 1995.
[2] J. Laskar and P. Robutel, Cel. Mech. Dyn. Astr. 80, 39, 2001.
[3] L. Nadolski, Ph. D. Thesis (Univ. Paris XI, 2001).
[4] L. Nadolski and J. Laskar, EPAC 2002, 1276, 2002.
[5] E. Forest and R. D. Ruth, Physica D 43, 105, 1990.
[6] Ch. Skokos, Y. Papaphilippou and J. Laskar, in preparation.
[7] M.Korostelev, PhD thesis, EPFL, 2006.
[8] Y. Papaphilippou, et al, these proceedings.
[9] http://mad.home.cern.ch/mad/